A Signature Correlation Study of Ground Target VHF/UHF ISAR Imagery

A. J. Gatesman[*a], C. Beaudoin[a], R. H. Giles[a], W. T. Kersey[a], J. Waldman[a], S. Carter[b], and W. E. Nixon[b]

[a]Submillimeter-Wave Technology Laboratory, University of Massachusetts Lowell
Lowell, MA 01854

[b]U.S. Army National Ground Intelligence Center, 2055 Boulders Road
Charlottesville, VA 22911

ABSTRACT

VV and HH-polarized radar signatures of several ground targets were acquired in the VHF/UHF band (171-342 MHz) by using 1/35th scale models and an indoor radar range operating from 6 to 12 GHz. Data were processed into medianized radar cross sections as well as focused, ISAR imagery. Measurement validation was confirmed by comparing the radar cross section of a test object with a method of moments radar cross section prediction code. The signatures of several vehicles from three vehicle classes (tanks, trunks, and TELs) were measured and a signature cross-correlation study was performed. The VHF/UHF band is currently being exploited for its foliage penetration ability, however, the coarse image resolution which results from the relatively long radar wavelengths suggests a more challenging target recognition problem. One of the study's goals was to determine the amount of unique signature content in VHF/UHF ISAR imagery of military ground vehicles. Open-field signatures are compared with each other as well as with simplified shapes of similar size. Signatures were also acquired on one vehicle in a variety of configurations to determine the impact of minor target variations on the signature content at these frequencies.

Keywords: VHF, UHF, radar, signature, FOPEN, correlation, imagery, decoy

1. INTRODUCTION

For the past twenty years, Expert Radar Signature Solutions (ERADS) under funding from the National Ground Intelligence Center (NGIC) has developed state-of-the-art scale model measurement systems to acquire radar signatures in support of a number of advanced radar applications such as automatic target recognition (ATR) systems, low-observable target evaluation, foliage penetration (FOPEN), RAM development, and buried object detection. ERADS has developed fully polarimetric compact ranges at 160 GHz[1], 520 GHz[2], and, 1.56 THz[3] for acquisition of X-band, Ka-band, and W-band radar imagery of 1/16th and 1/48th scale model targets and scenes. Other radar bands have been simulated using appropriately scaled models.

[*] correspondence: email: andrew_gatesman@uml.edu; telephone: 978-458-3807; fax: 978-452-3333; web: http://stl.uml.edu; mail: Submillimeter-Wave Technology Laboratory, 175 Cabot Street, Suite 130, Lowell, MA 01854

Report Documentation Page

Form Approved
OMB No. 0704-0188

1. REPORT DATE	2. REPORT TYPE	3. DATES COVERED
SEP 2003		**00-00-2003 to 00-00-2003**

4. TITLE AND SUBTITLE	5a. CONTRACT NUMBER
A Signature Correlation Study of Ground Target VHF/UHF ISAR Imagery	5b. GRANT NUMBER
	5c. PROGRAM ELEMENT NUMBER
6. AUTHOR(S)	5d. PROJECT NUMBER
	5e. TASK NUMBER
	5f. WORK UNIT NUMBER
7. PERFORMING ORGANIZATION NAME(S) AND ADDRESS(ES) **University of Massachusetts Lowell,Submillimeter-Wave Technology Laboratory,175 Cabot Street,Lowell,MA,01854**	8. PERFORMING ORGANIZATION REPORT NUMBER
9. SPONSORING/MONITORING AGENCY NAME(S) AND ADDRESS(ES)	10. SPONSOR/MONITOR'S ACRONYM(S)
	11. SPONSOR/MONITOR'S REPORT NUMBER(S)

12. DISTRIBUTION/AVAILABILITY STATEMENT
Approved for public release; distribution unlimited

13. SUPPLEMENTARY NOTES
The original document contains color images.

14. ABSTRACT

15. SUBJECT TERMS

16. SECURITY CLASSIFICATION OF:			17. LIMITATION OF ABSTRACT	18. NUMBER OF PAGES	19a. NAME OF RESPONSIBLE PERSON
a. REPORT **unclassified**	b. ABSTRACT **unclassified**	c. THIS PAGE **unclassified**		**12**	

Recently, there has been a resurgence in interest in developing radar systems capable of detecting, classifying, and potentially identifying military targets obscured by foliage. Such systems typically operate at VHF or UHF frequencies to penetrate vegetation canopies and use large fractional bandwidths ($\Delta f / f_c \geq 100\%$) coupled with large synthetic apertures (20°-90° aspect swaths) to maximize image resolution.

VHF and UHF frequencies may have the significant operational advantage of only weakly backscattering from rough terrain and propagating with little attenuation through foliage, however, the application of longer wavelengths result in coarser ISAR image resolution. Typical imagery contains fewer than 50 resolution cells on target and tree trunks still remain as large scatterers. Solving the automatic target recognition problem at frequencies below 1 GHz may prove more challenging than at higher radar frequencies and at some lower frequency, target recognition may not be feasible.

In response to the growing interest in detecting and potentially identifying targets under trees, STL is developing a scale modeling program aimed at gathering radar scattering characteristics of targets in forested areas. STL has developed the capability for acquiring VHF/UHF signatures by using a microwave radar system and scale models situated on dielectrically scaled ground terrain and obscured by dielectrically scaled trees[4]. This study's main focus was to determine the amount of unique signature content that exists in VHF/UHF ISAR imagery of military ground vehicles by building a well-documented library of calibrated imagery on a variety of targets. Signatures were acquired on an array of 10 targets at 20°, 30°, and 40° elevation and processed into focused, inverse synthetic aperture imagery. Images were compared by calculating the correlation coefficient between several pairs of images. To facilitate the study, signatures were acquired with targets placed on a smooth, dielectric ground plane without trees. While the measurements are fully polarimetric, the correlation studies reported in Section 5 involved only HH and VV imagery.

2. MEASUREMENT SYSTEM AND SCALE MODELS

The signature acquisition system consisted of a microwave transceiver, target/calibration positioning stage, and a data acquisition and processing computer (Fig. 1). The transceiver was based on an Agilent microwave vector network analyzer and consisted of a 8341B microwave source, 8511A frequency converter, and a 8510C network analyzer.

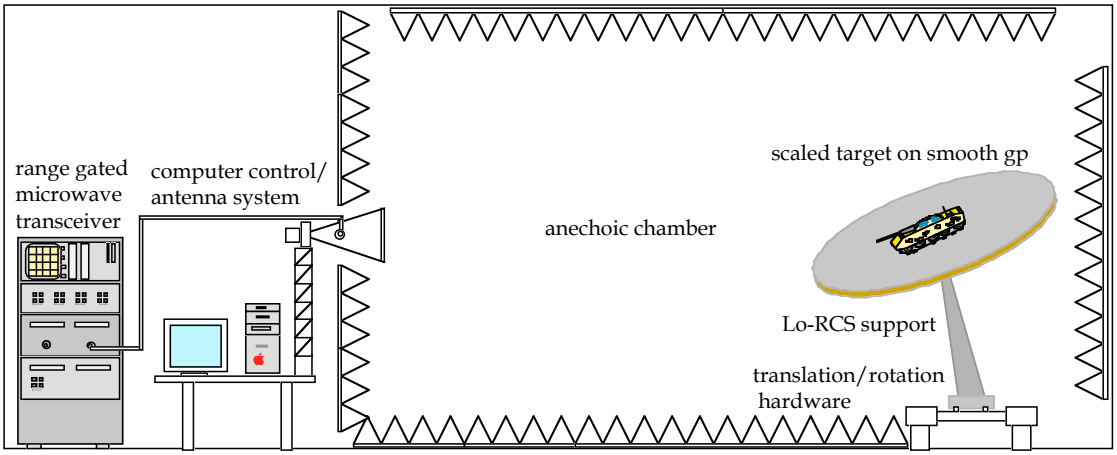

Figure 1: Microwave radar system used for acquisition of VHF/UHF signatures of scale model targets.

2.1. System Hardware and Measurement Procedure

Signature measurements involved stepping the transmitted frequency over the system's operational bandwidth (6-12 GHz) while the receiver recorded the magnitude and phase of the backscattered signal from the scale model scene for each linear polarization state. Due to the monostatic configuration of the system, wideband circulators were necessary to separate transmit and receive signals. Due to the circulator's limited ability to isolate outgoing and incoming signals (-25 dB isolation), a pulse modulation (hardware range gating) system was developed by incorporating fast pin diode switches. Fast switching permitted the receiver to be disconnected from the transmit pulse (-80 dB isolation) and subsequently switch on only when backscattered energy was expected from the target under test. Hardware gating also prevented clutter from other areas of the chamber from being measured.

The procedure was repeated for each desired aspect angle of the target and scene. Prior to acquiring data on a target, a background frequency sweep was collected with the target and calibration objects both removed from the chamber. Next, a flat plate of known radar cross section was translated into the beam and a second frequency sweep was acquired. Finally, a dihedral was measured. The background sweep was then coherently subtracted from the flat plate and dihedral data. The plate and dihedral data (with background now removed) were compared to their theoretical responses and used to obtain a polarimetric normalization array, which was subsequently applied to each target frequency sweep. Finally, a correction for the beam divergence was applied to the data to account for the fact that the target and calibration objects were at different distances from the stationary radar antenna. The result was a fully calibrated frequency sweep. Prior to image processing, software range gating was applied to the calibrated frequency data. Due to the system's hardware gating capability, software range gating was not absolutely necessary, but did offer additional suppression of clutter in the target receive gate.

The transmit horn was a Condor Systems 2-18 GHz quadridged horn. To enhance the gain of the horn, a hyperbolic/flat lens was positioned approximately 8 inches from the horn's aperture The combination of the lens and horn resulted in a ≈ 4.3-in.-radius gaussian beam waist ($1/e^2$ power) at the len's output aperture. The radiation was allowed to expand as a spherical-gaussian beam out to the target under test. The target was placed in the far-field of the transmitting horn. A 5-axis computer-controlled stage was used to control the position of the target and calibration objects. Three axes controlled the translation, azimuth, and elevation of the ground plane / target scene and two axes positioned a flat plate and dihedral used for polarimetric calibration.

2.2. Scale Model Targets and Ground Plane

Ten $1/35^{th}$ scale targets (Figs. 2 and 3) were used in the study and are listed in Table I. All of the targets, except the M1 tank, were spray coated with a high conductivity, silver-loaded paint (DuPont # 4817N). An average electrical conductivity of ≈ 9 x 10^{14} s^{-1} was measured using several paint samples and a 4-point resistivity probe. Even though a bulk metal has a conductivity of ≈ 3 x 10^{17} s^{-1}, the paint's conductivity was more than sufficient to be highly reflective (R > 98%) in the 6-12 GHz band. The M1 tank was coated with 4000Å of copper. Assuming that copper film's resistivity was no more than 10x higher than its bulk value, the 6-12 GHz reflectivity was ≥ 99%. Two simplified shapes; a solid aluminum block and a decoy, were also included in the signature study. Both simplified shapes were constructed to have approximately the same footprint as the tanks. A full scale decoy was assumed to be constructed from standard dimensional lumber and metallic wire mesh. The scale model was constructed using balsa wood to simulate the dielectric behavior of construction lumber and a metal mesh of an appropriate aperture size was used.

Table I. 1/35th scale targets used in the signature correlation study.

Simplified Shapes	Trucks	Main Battle Tanks	TELs, APCs
		M1	
Al block	Gaz 66	T72	SCUD
Decoy	M35	T80	M2A2
		T80 ERA	

Figure 2: 5 of the 10 targets used in the signature correlation study. From left to right; Al block, Decoy, Gaz 66 truck , M35 truck, and a M2A2 Bradley armored personnel carrier.

Figure 3: 5 of the 10 targets used in the signature correlation study. From left to right; SCUD TEL, M1 tank, T72 tank, T80 tank, and a T80 tank with ERA (explosive reactive armor).

Signature data were acquired with targets placed on a smooth, 4-ft.-diameter dielectric ground plane. Scale modeling requires that the 6-12 GHz dielectric constant of the model ground equal the dielectric constant of actual soil at VHF/UHF frequencies. By using a graphite-loaded polyurethane resin, a dielectric constant of □□ 20 + j 2.5 at 9 GHz was achieved which models soil with a typical moisture content.

3. RCS MEASUREMENT VALIDATION

RCS measurement accuracy was demonstrated by making a series of measurements on a metallic test object known as Slicy (Fig. 4) which is comprised of a variety of simple shapes such as dihedrals, trihedrals, and cylinders. A method of moments electromagnetics prediction code (Carlos) was used to predict the X-band RCS of the target for comparison with laboratory measurements. Slicy was mounted on a low-RCS pylon at 15° elevation and its 10 GHz (286 MHz full scale) RCS was measured over a 360° azimuth sweep. Excellent agreement (Fig. 5) was observed between data and prediction for all four polarizations.

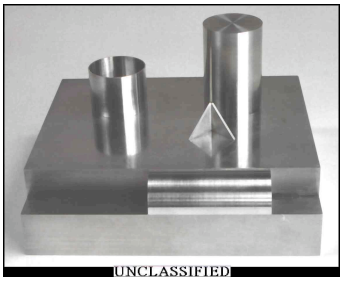

Figure 4: Scale model Slicy used to validate STL's VHF/UHF measurement capability. The base of the model is approx. 7 in. x 7 in.

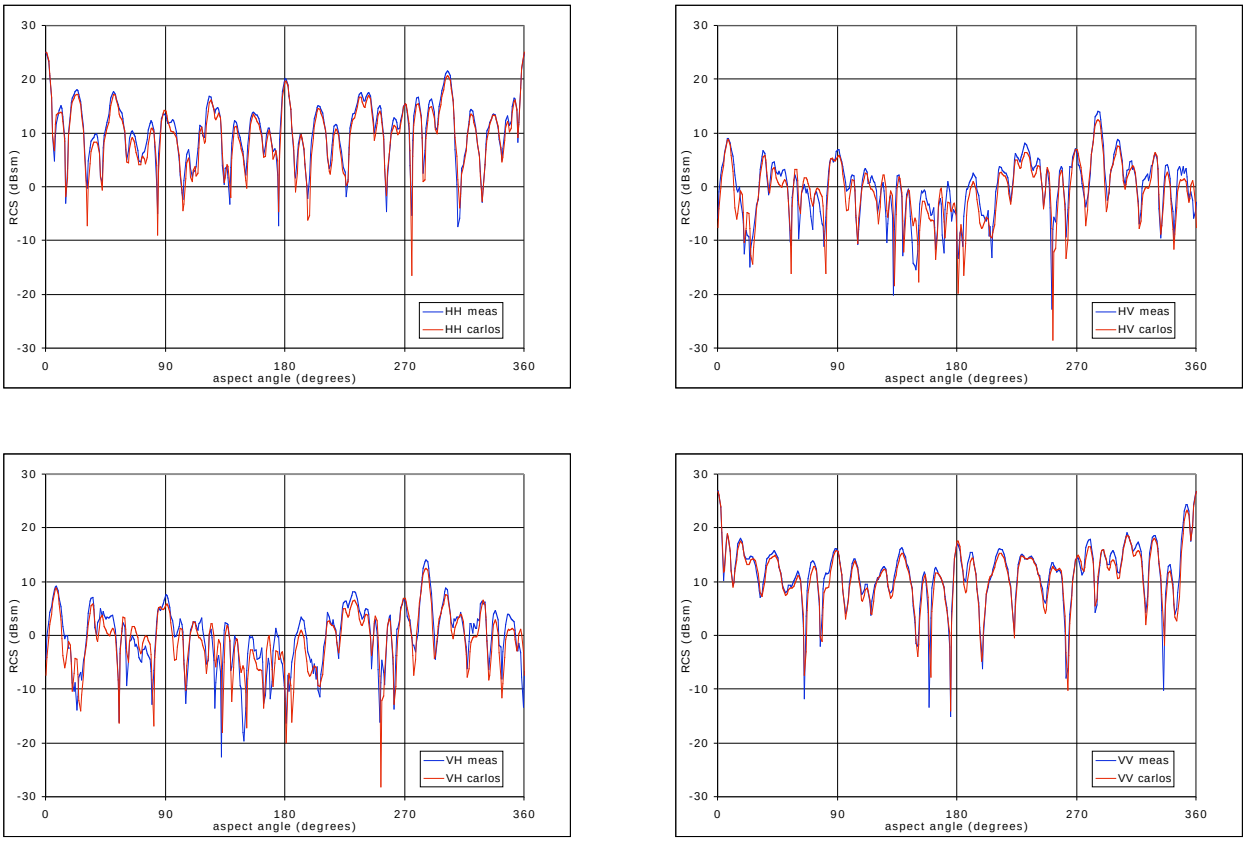

Figure 5: Polarimetric RCS of Slicy at 286 MHz. (The data have been adjusted to represent VHF/UHF data by assuming the model in Fig. 4 was a 1/35th scale Slicy, i.e. 10log(35^2) was added to the measured RCS).

4. VHF/UHF DATA ACQUISITION AND IMAGE PROCESSING

360° aspect spins were acquired for each target at three elevation angles; 20°, 30°, and 40°. The radar cross sections (units of dBsm) were calculated for each vehicle at each elevation angle (Table II). The data in Table II were calculated by first averaging the 64 RCS (in m^2) vs aspect arrays which remained after software range gating, and then calculating the median value (in dBsm) of the averaged array. Though the aluminum block had nearly the same footprint as the vehicles, its median RCS was lower than all other vehicles. The decoy, however, had a RCS which was quite close to the RCS of the ground vehicles. The effects of the ground plane's Brewster angle ($\approx$ 13° elevation) was apparent in the VV data. As the elevation angle was increased from 20° to 40°, the target's VV RCS also tended to increase.

Table II. Medianized radar cross section (dBsm) averaged over the 171-342 MHz bandwidth.

elev. angle	pol.	Al block	Decoy	Gaz 66	M1	M2A2	M35	SCUD	T72	T80	T80 ERA
20°	HH	8.5	11.8	9.7	10.1	9.7	10.3	13.4	10.6	11.6	12.3
	VV	0.5	5.3	5.5	7.1	5.3	8.6	8.3	6.7	7.3	6.9
30°	HH	7.9	11.5	9.3	10.2	8.9	9.6	12.1	10.4	10.1	11.1
	VV	3.9	6.8	6.4	8.3	6.9	10.2	9.5	7.0	7.6	7.6
40°	HH	7.5	11.0	9.0	10.0	8.5	8.3	11.7	8.9	10.2	9.4
	VV	4.4	7.8	6.6	8.8	7.4	9.7	8.9	7.9	8.6	7.8

In order to form an ISAR image of reasonable resolution ($\approx$ 1 m^2 resolution cells full scale), the full 6 GHz frequency bandwidth (equivalent to 171 MHz of bandwidth full scale) and 40° angular swaths of data were coherently processed. Processing over a large region in the spatial frequency domain and the desire to use computationally efficient FFT processing, required the use of focusing techniques, which, if not used, would result in a blurred image.[5] One common technique for forming focused ISAR imagery is to apply a polar-to-rectangular resampling algorithm[6] to the data. The goal is to properly remap the acquired polar formatted data onto a rectangular raster upon which two one-dimensional Fourier transforms can be independently applied in the range and cross-range directions.

360 slant-plane ISAR images (one for each aspect angle) were formed for each target at 20°, 30°, and 40° elevation. Representative imagery are shown in Figs. 6-9. Image pixel size is approximately 0.2 m^2 whereas actual image resolution cell size is 1 m^2. The images have 26 dB of dynamic range and a –27 dBsm threshold was used (i.e. black pixels are –27 dBsm). Figure 6 shows ISAR imagery for the M1 Abrams main battle tank and the Russian T72 main battle tank. Even though image resolution was limited to 1 m^2, the imagery show a significant amount of unique signature content associated with each target. Figure 7 shows the Decoy and T80 with ERA at 30° elevation and 210° aspect. Even though these targets had very similar medianized radar cross sections, their imagery clearly displayed distinct features. Images are shown in Figs. 8 and 9 for the M35 truck, Gaz 66 truck, M2A2 Bradley, and SCUD.

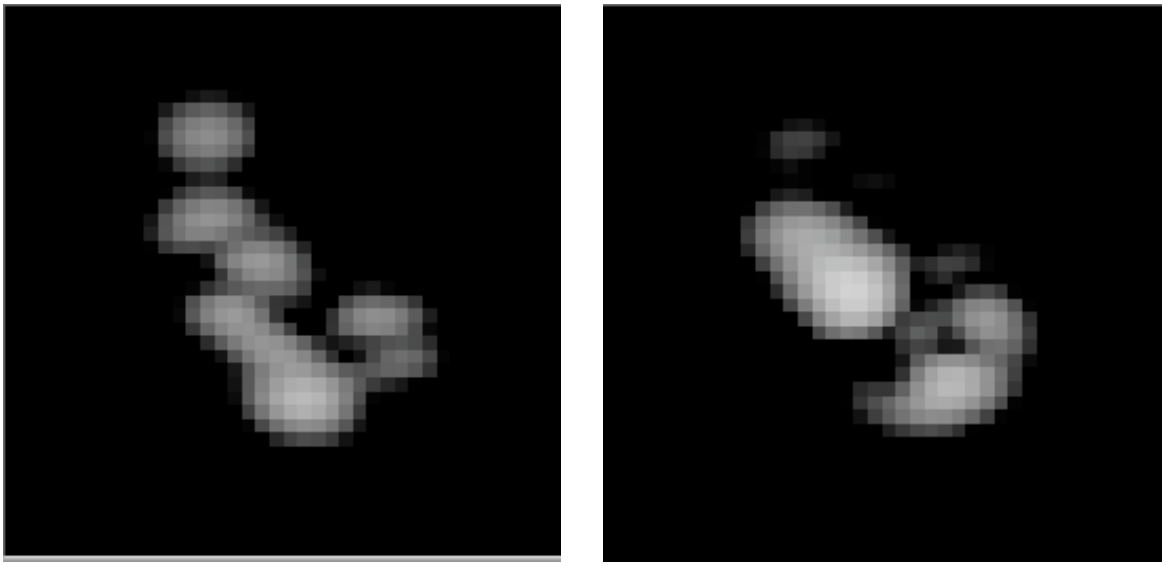

Figure 6: HH ISAR imagery of a M1 tank (left) and a T72 tank (right) at 30 degrees elevation and 210° aspect. Distinct features are clearly observed in the 1m x 1m resolution imagery.

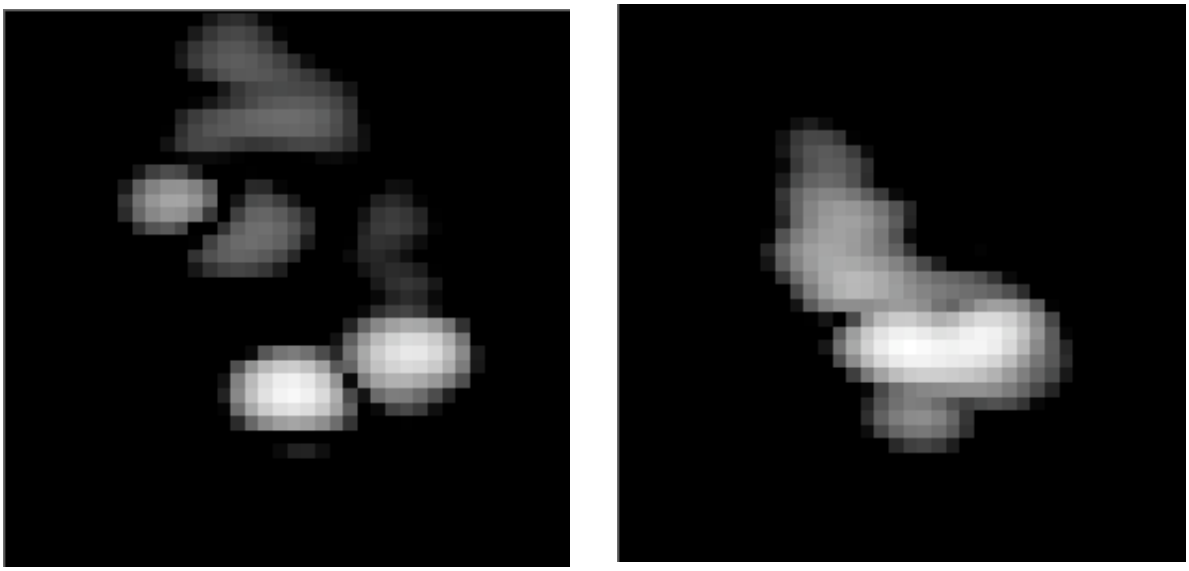

Figure 7: HH ISAR imagery of the Decoy (left) and a T80 tank with ERA (right) at 30 degrees elevation and 210° aspect. The two bright scatterers seen in the Decoy image are the two leading corners of that target. Some downrange scattering can be observed as well and most likely is due to multibounce within the Decoy's cavity.

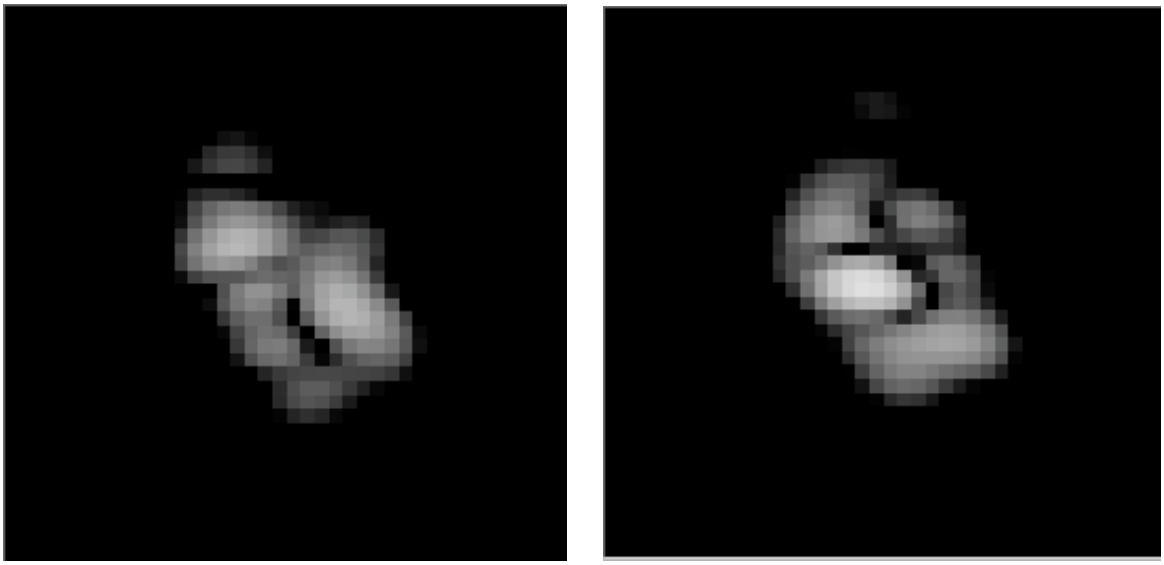

Figure 8: HH ISAR imagery of a M35 truck (left) and a Gaz 66 truck (right) at 30 degrees elev. and 210° aspect.

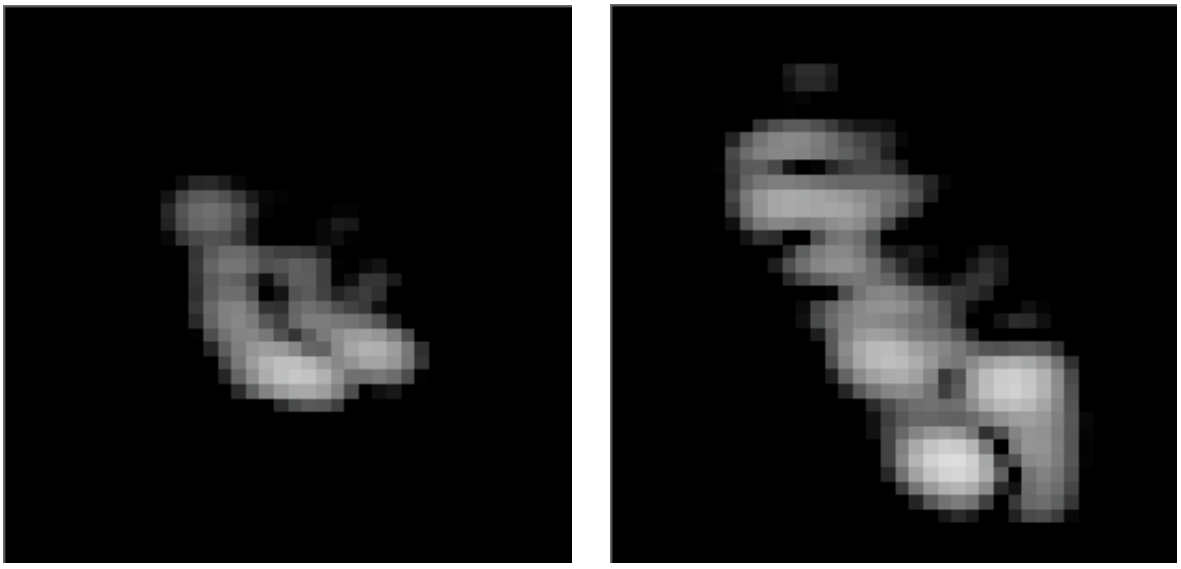

Figure 9: HH ISAR imagery of a M2A2 Bradley (left) and a SCUD TEL (right) at 30 degrees elev. and 210° aspect.

5. CROSS-CORRELATION OF VHF/UHF ISAR IMAGERY

5.1. Cross-Correlation Algorithm

The autonomous nature of the signature acquisition system permitted rapid population of a VHF/UHF imagery library from which a comprehensive signature correlation study was performed. The algorithm used was a standard two-dimensional correlation technique[7] and has been successfully applied to scale model W-band data.[8] The basic algorithm is given by:

{ EMBED Equation.3 }

$$h(s,t) = \frac{\sum_x \sum_y [f(x,y) - \bar{f}(x,y)][g(x-s, y-t) - \bar{g}]}{\{\sum_x \sum_y [f(x,y) - \bar{f}(x,y)]^2 \sum_x \sum_y [g(x-s, y-t) - \bar{g}]^2\}^{1/2}} \quad . \qquad \text{Eq. (1)}$$

The functions *f(x,y)* and *g(x,y)* represent the two images to be compared and *h(s,t)* is a normalized correlation coefficient with a maximum value of unity (100%) when the images are perfectly correlated. The procedure for correlating a pair of ISAR images consisted of first thresholding all pixels to a particular level and subsequently adding the absolute value of the threshold value to all pixels. This step ensured that the minimum pixel value was 0 dBsm so that noise and other low-level image artifacts would carry zero weight in the correlation. As one of the images was incrementally positioned over the other, a single correlation coefficient was calculated using Eq. (1). A two-dimensional array of coefficients *h(s,t)* was generated from which the maximum value was retained. This procedure was repeated for all 360 aspect angles associated with a given pair of targets. The 360 coefficients were plotted as a function of aspect angle and a probability density was formed. A typical correlation (expressed in percent) and probability density plot are shown in Fig. 10 for a T80 tank with and without explosive reactive armor.

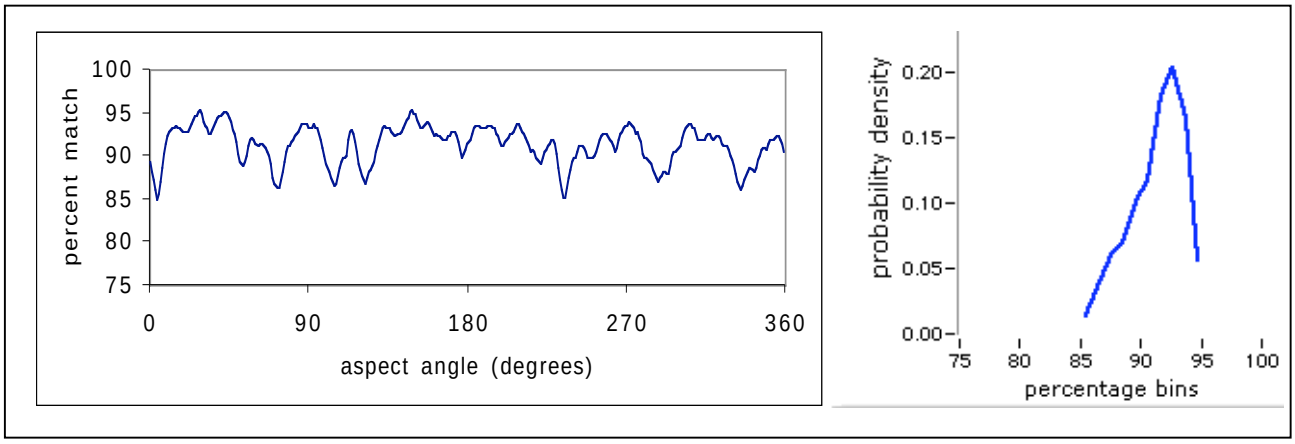

Figure 10: Typical correlation data (T80 vs T80 with ERA) presented as a percent match vs aspect angle and in histogram format.

5.2. System and Calibration Stability Testing

Before performing the cross-correlation study, several tests were conducted to determine the overall signature-to-signature measurement stability of the system. The T72 was chosen as the test target. The first test consisted of collecting data for two sequential 360° spins. Correlation of the two datasets was expected to be very good with nearly 100% match at each aspect angle. The second test consisted of waiting a day between two nominally identical spins but reusing the same calibration. Such a test would reveal any time-dependent changes in the system's calibration. A third test consisted of two sequential measurements, but prior to the second spin, the target was removed and replaced on the ground plane revealing the correlation's sensitivity to slight target repositioning. Results of the sensitivity tests demonstrate excellent system, calibration, and positional stability for both HH and VV polarizations and are summarized for HH in Table III.

Table III. Sensitivity testing of the measurement system.

30°, HH	T72 spin 2	T72 next day	T72 after move
T72 spin 1	99.7	99.4	
T72 spin 2		99.4	
T72 before move			99.4

5.3. Correlation Results

Cross-correlation results for the ten target signature study are shown in Table IV for HH polarization and 20° elevation. No dependence on elevation angle was observed. Correlation coefficients were all > 83% except for the comparison involving the aluminum block, decoy, and the SCUD. Poor correlation with the SCUD is not surprising as Eq. (1) mainly behaves as a spatial correlator. However, the very poor correlation with the simplified shapes only emphasizes the level of unique signature content that still must exist in this relatively low frequency imagery.

The correlation coefficient was observed to be slightly dependent on polarization. In nearly all cases, the VV imagery tended to decorrelate more than the HH imagery. The differences in the HH and VV response are shown in Table V and represent differences after averaging over the three elevation angles.

Table IV. HH signature correlation results (in percent) for 10 targets at 20° elevation.

20°, HH	Decoy	Gaz 66	M1	M2A2	M35	SCUD	T72	T80	T80 ERA
Al block	80.1	60.8	74.0	70.1	61.9	62.9	68.9	67.3	68.1
Decoy		66.9	77.1	73.4	69.4	74.5	76.3	74.6	74.4
Gaz 66			83.5	87.7	90.4	73.2	85.7	87.7	88.1
M1				89.4	85.3	79.8	89.0	87.9	87.4
M2A2					88.3	76.0	88.9	89.4	89.1
M35						77.2	87.0	88.3	88.9
SCUD							80.5	77.9	77.6
T72								89.7	89.2
T80									91.3

Table V. Percent difference between HH and VV signature correlations averaged over 3 elevation angles.

HH - VV	Decoy	Gaz 66	M1	M2A2	M35	SCUD	T72	T80	T80 ERA
Al block	8.0	0.3	7.3	4.1	0.9	3.2	4.2	4.3	3.6
Decoy		1.4	5.6	4.0	1.3	6.4	4.7	4.1	4.0
Gaz 66			-1.1	0.6	3.1	3.0	1.0	0.5	1.5
M1				1.1	-0.4	3.7	1.7	0.8	0.4
M2A2					2.5	2.2	2.1	1.0	1.1
M35						3.1	0.7	1.0	1.9
SCUD							3.4	3.6	3.8
T72								1.7	1.9
T80									1.5
T80 ERA									

5.4. Separability of M1 and T80 VHF/UHF imagery

Of interest to the automatic target recognition community is the ability to correctly identify a target by its radar signature. A primary interest is the degree to which imagery from a target such as a M1 looks like imagery from a similar vehicle such as a T80. In particular, how rapid does a target's imagery decorrelate with itself when the target's configuration is modified or altered as it may be when used in a realistic condition? Scale model signatures are ideally suited to perform such a study. A scale model T80 was measured in a variety of configurations (untouched, turret turned 10°, fuel drums removed, fuel drums and snorkel removed) and an intra-target correlation analysis was performed. The various T80 imagery were also compared with M1 imagery. Percent matches averaged over 360° aspect spin are shown in Table VI. For each altered T80 compared with an untouched T80, correlations were $\geq$ 95% or better. When compared with a M1, however, correlation coefficients fell below 90%.

Table VI. Correlation of several T80 configurations compared with an M1.

20°, HH	T80	T80 10° turret	T80 fuel drums removed	T80 fuel drums and snorkel removed
T80		94.9	98.5	97.2
M1	87.8	88.0	87.9	87.5

Signature separability, however, is more accurately gauged by plotting a histogram of correlation values. Fig. 11 shows probability density functions of the various correlations between the T80 and M1 depicted in Table VI. By "jettisoning" various components from the T80 (fuel drums, snorkel), only a slight impact was observed when correlated with an untouched T80. Rotating the turret 10° had the greatest impact and dropped the average percent match to 95%. However, when the M1 tank imagery was compared with each of the four T80 configurations, a much greater decorrelation was observed. Fig. 11 demonstrates a clear separation between the T80 and M1 probability density functions. Such results support the notion that some level of target identification at these frequencies may be feasible.

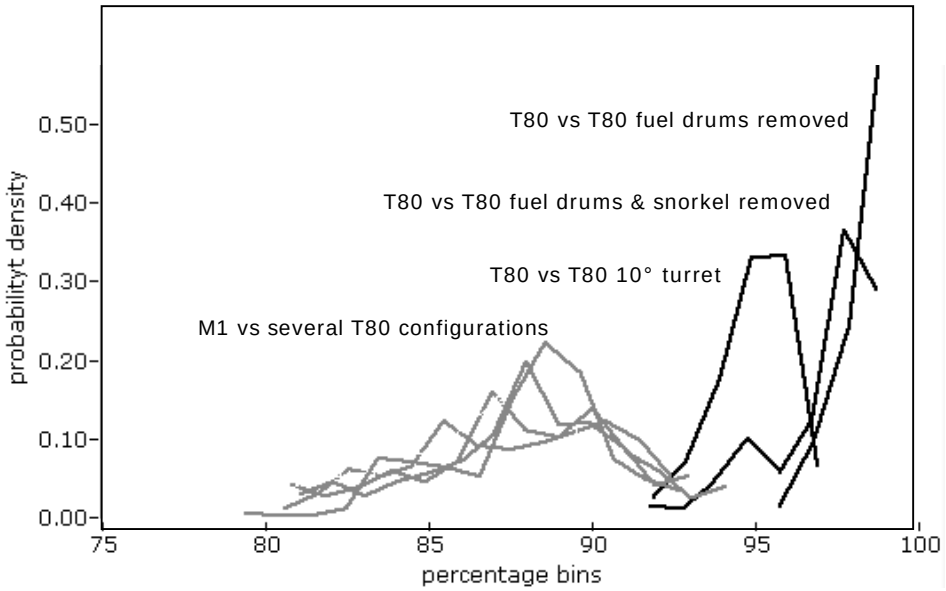

Figure 11: Probability density functions depicting the correlation between an M1 tank and various configurations of a T80.

6. SUMMARY

A radar range was developed for acquisition of 171–342 MHz imagery of ground targets by using a 6-18 GHz radar range and 1/35th scale model targets. Accuracy of RCS measurements was validated by comparing polarimetric data acquired on a metallic test shape with method of moments electromagnetic predictions. The radar signatures of 8 scale model ground targets and two simplified shapes were measured every degree over a 360° aspect spin at 20°, 30°, and 40° elevation. Data were processed into focused ISAR imagery. A correlation study was performed on the imagery to ascertain the amount of unique signature content in the images. Distinct differences in the two-dimensional imagery of similar-sized targets were readily observable. A specific study comparing a M1 tank with several reconfigured T80 tanks suggests that signature separability may be feasible for like-sized targets at these frequencies.

REFERENCES

1. M. J. Coulombe, T. Horgan, J. Waldman, J. Neilson, S. Carter, and W. Nixon, "A 160 GHz Polarimetric Compact Range for Scale Model RCS Measurements," Antenna Measurements and Techniques Association (AMTA) Proceedings, Seattle, WA, October 1996.

2. M. J. Coulombe, T. Horgan, J. Waldman, G. Scatkowski, and W. Nixon, "A 520 GHz Polarimetric Compact Range for Scale Model RCS Measurements," Antenna Measurements and Techniques Association (AMTA) Proceedings, Monterey, October 1999.

3. T. M. Goyette, J. C. Dickinson, J. Waldman, W. E. Nixon, and S. Carter, "Fully Polarimetric W-band ISAR Imagery of Scale-Model Tactical Targets Using a 1.56 THz Compact Range," Proceeding of SPIE 15th Annual International Symposium on Aerospace/Defense, Simulation, and Controls, Vol. 4382, Orlando, FL, April 2001.

4. A. J. Gatesman, C, Beaudoin, R, Giles, J. Waldman, and W. E. Nixon, "VHF/UHF Imagery and RCS Measurements of Ground Targets in Forested Terrain," Proceeding of SPIE 16th Annual International Symposium on Aerospace/Defense, Simulation, and Controls, Vol. 4727, Orlando, FL, April 2002.

5. D. L. Mensa, *High Resolution Radar Cross-Section Imaging*, Artech House, Inc. Norwood, MA 1991.

6. C. V. Jakowatz, et. al., *Spotlight-Mode Synthetic Aperture Radar: A Signal Processing Approach*, Kluwer Academic Publishers, 1996.

7. R. C. Gonzalez and R. E. Woods, *Digital Image Processing*, Addison-Wesley Publishing Company, 1993.

8. T. M. Goyette, J. C. Dickinson, R. H. Giles, W. T. Kersey, J. Waldman, and W. E. Nixon, "Analysis of Fully-Polarimetric W-Band ISAR Imagery on Seven Scale-Model Main Battle Tanks for Use in Target Recognition," Proceeding of SPIE 16th Annual International Symposium on Aerospace/Defense, Simulation, and Controls, Vol. 4727, Orlando, FL, April 2001.